

Compensation for Booster Leakage Field in the Duke Storage Ring ^{*}

Wei Li^{1,2;1)} Hao Hao^{2,2)} Stepan F. Mikhailov² Victor Popov²
Wei-Min Li¹ Ying K. Wu²

¹ National Synchrotron Radiation Laboratory, University of Science and Technology of China, Hefei, 230029, China

² Triangle University Nuclear Laboratory/Physics Department, Duke University, Durham, 27705, USA

Abstract: The High Intensity Gamma-ray Source (HIGS) at Duke University is an accelerator-driven Compton gamma-ray source, providing high flux gamma-ray beam from 1 MeV to 100 MeV for photo-nuclear physics research. The HIGS facility operates three accelerators, a linac pre-injector (0.16 GeV), a booster injector (0.16–1.2 GeV), and an electron storage ring (0.24–1.2 GeV). Because of proximity of the booster injector to the storage ring, the magnetic field of the booster dipoles close to the ring can significantly alter the closed orbit in the storage ring being operated in the low energy region. This type of orbit distortion can be a problem for certain precision experiments which demand a high degree of the energy consistency of the gamma-ray beam. This energy consistency can be achieved by maintaining consistent aiming of the gamma-ray beam, therefore, a steady electron beam orbit and angle at the Compton collision point. To overcome the booster leakage field problem, we have developed an orbit compensation scheme. This scheme is developed using two fast orbit correctors and implemented as a feedforward which is operated transparently together with the slow orbit feedback system. In this paper, we will describe the development of this leakage field compensation scheme, and report the measurement results which have demonstrated the effectiveness of the scheme.

Key words: field compensation, feedforward, storage ring, beam orbit

PACS: 29.20.db

1 Introduction

The High Intensity Gamma-ray Source (HIGS) at Duke University is an accelerator-driven Compton gamma-ray source for photo-nuclear research. It provides a very high intensity gamma-ray beam with switchable polarization in the energy range from 1 MeV to 100 MeV. The HIGS facility consists of three accelerators: a linac pre-injector (0.16 GeV), a booster injector (0.16–1.2 GeV), and an electron storage ring (0.24–1.2 GeV) [1, 2], as shown in Fig. 1. The 34-meter-long south straight section hosts the Duke Free-Electron Lasers (FELs) with several undulator configurations, producing an FEL beam with wavelength ranging from 190 nm to 2 μm [3]. The FEL beam is trapped in a 53.73 m long low-loss laser cavity to be synchronized with the circulating electron beam (2.79 MHz). Operating in the two-bunch mode with two electron bunches separated by a half of the storage ring circumference from each other, a high flux gamma-ray beam is produced in the middle of the south straight section by colliding one electron bunch

head-on with the high power FEL beam produced by the other electron bunch [4, 5]. After collimated by the downstream collimator, the gamma-ray beam becomes quasi-monochromatic and is delivered to the target room.

However, due to the proximity of the booster injector to the storage ring, the magnetic field of the booster dipoles close to the storage ring can significantly alter the closed orbit in the storage ring when being operated in the low energy region. The resulted beam orbit distortion can be a significant problem for low energy gamma-ray production, which requires consistent aiming of the gamma-ray beam, therefore, a steady electron beam orbit in the collision area. This kind of disturbance can be a problem for similar accelerator facilities in which the booster injector shares the same tunnel with the storage ring [6, 7]. This kind of problem is also very important for the next generation light source, e.g. diffraction limited storage ring (DLSR) [9], since electron beams in the DLSR can be sensitive to the integrated magnetic field variation on the level of 10^{-6} T·m. Therefore, it is important to develop shielding or compensation schemes

Received XX XXX 2016

* Supported by National Natural Science Foundation of China (11175180, 11475167) and US DOE (DE-FG02-97ER41033)

1) E-mail: wei.li3@duke.edu

2) E-mail: hhao@fel.duke.edu

©2013 Chinese Physical Society and the Institute of High Energy Physics of the Chinese Academy of Sciences and the Institute of Modern Physics of the Chinese Academy of Sciences and IOP Publishing Ltd

for the leakage magnetic field from a nearby ramping booster [6, 8].

At the HIGS facility, during routine operation the electron beam is first injected into the booster at 169 MeV, the booster is then ramped to bring the electron beam to the extraction energy (any where between 240 MeV and 1.2 GeV), the electron beam is extracted into the storage ring, and finally the booster is ramped up to the maximum energy of 1.2 GeV and then down to 169 MeV to finish one injection cycle. In this process, it is observed that the beam orbit in the storage ring is significantly affected by the booster leakage field, as shown

in Fig. 2. For gamma-ray operation above about 15 MeV, Compton scattered electrons lose too much energy so that they cannot be retained in the storage ring [10]. In this electron loss mode, continuous electron beam injection into the storage ring is needed to compensate for a high rate of electron loss. In this mode, the amount of time during which the collision orbit is altered due to the periodic booster ramping becomes a significant portion of the gamma-ray production. The adverse impact of the booster leakage field is most significant for the Compton gamma-ray production using a low energy electron beam below 600 MeV.

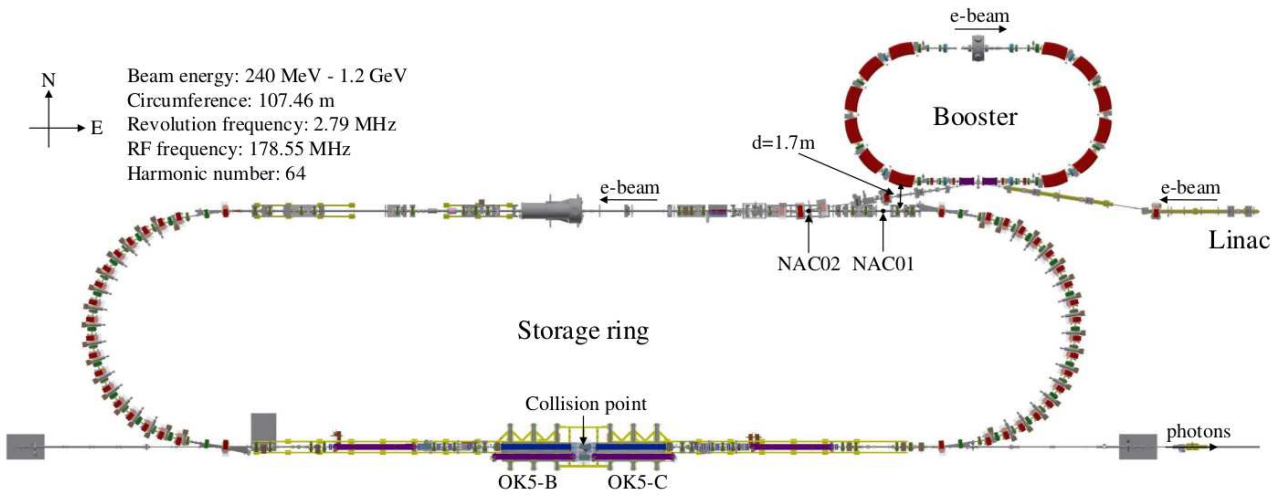


Fig. 1. The layout of Duke storage ring and its booster injector. The closest booster dipole magnet is about 1.7m away from the nearby storage ring beam line.

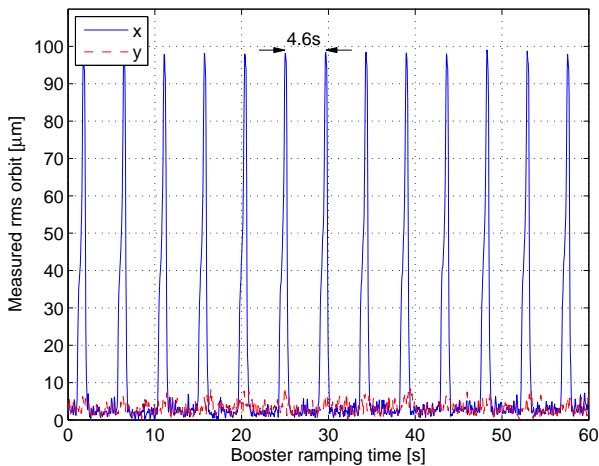


Fig. 2. (color online) The measured rms beam orbit deviations in the storage ring as a function of time while continuously ramping the booster with a repetition rate 4.6 s. The storage ring is operated at $E_{SR} = 426$ MeV.

To obtain a consistent collision orbit for the gamma-

ray operation, an orbit compensation scheme for the booster leakage field is developed. This scheme is devised using a beam based technique with two air coil correctors, and implemented as a feedforward system which is operated transparently together with the slow orbit feedback system. In this paper, we will present the development of the orbit compensation scheme for the booster leakage field, and report the measurement results of this compensation in two different modes: (1) the static mode of operation while stepping the booster energies, and (2) the dynamic mode of operation with continuous booster ramping.

2 Field leakage compensation scheme

The closed orbit in a circular accelerator is determined by the magnetic field (i.e. in magnets) and electric field (e.g. in the RF cavity) around the accelerator, which can be distorted by the field errors. To control the orbit distortions caused by slow and distributed magnetic field errors, a slow orbit feedback is commonly employed,

in which the corrector strengths are calculated based on the beam orbit deviations measured using beam position monitors (BPMs) and a pre-measured response matrix.

At the Duke storage ring (DSR), the slow orbit feedback system is composed of 55 horizontal correctors, 24 vertical correctors and 32 BPMs [11]. It is operated at 1 Hz, which is fast enough to correct the orbit distortions caused by slow varying errors, e.g. those associated with temperature changes and slow power supply drifts. For the booster injector, the full energy ramp up and down cycle takes about 1.2 s to complete, hence it is not feasible to control the orbit perturbation caused by the booster leakage field using the existing slow orbit feedback system. The fast orbit feedback operating at a few hundred or thousand Hz may be feasible for the booster orbit correction [12], but it requires a significantly investment on the electronics and vacuum system. Hence, an alternative economic compensation scheme is needed. Since the booster is located to the northeast of the storage ring, the leakage field is also confined to this area. To minimize the orbit perturbation outside of this area, some local correctors can be employed. Moreover, as the strength of the leakage field is repeatable and can be pre-determined, a feedforward correction scheme can be used. In this scheme, the corrector strengths can be determined in advance as a function of the leakage field strength or the booster energy, and correctors can be synchronized with the booster energy ramping.

In the HIGS operation, a nearly monochromatic gamma-ray beam is produced by sending the beam through a small collimator. The aiming of the gamma-ray beam is determined by the position and direction of the relativistic electron beam at the collision point. Therefore, to maintain the energy resolution of the gamma-ray beam, the change of the electron beam orbit (both displacement and angle) at the collision point must be kept small. For some electron beam displacement Δx_c and angular deviation $\Delta\theta_c$ at the collision point, the offset of the gamma-ray beam center Δx_{coll} at the location of the collimator is given by

$$\Delta x_{coll} = \Delta x_c + \Delta\theta_c \cdot L, \quad (1)$$

where $L = 53$ m is the distance between the collision point and the collimator. If we require Δx_{coll} to be less than 10% of the smallest collimator diameter (6 mm), the maximumly allowed electron beam displacement is $\Delta x_{coll,max} = 0.6$ mm, and the maximumly allowed angular variation is $\Delta\theta_{coll,max} = 11\mu\text{rad}$. Typically, the electron orbit displacement is small, the main problem is the change of the electron beam angle at the collision point, as its effect is significantly amplified by the large distance between the collision point and the location of the collimator ($L = 53$ m).

The perturbed orbit in the storage ring is measured

with the booster injector parked at 1.2 GeV (the maximum energy), as shown in Fig. 3. It is observed that the perturbation is mostly in the horizontal direction with the maximum offset of $179\mu\text{m}$ around the storage ring. In this case, the orbit displacement is about $115\mu\text{m}$ and angular variation is about $14\mu\text{rad}$ at the collision point. In vertical direction, the orbit perturbation is one order of magnitude smaller, which is too small to be a problem. Thus, the compensation scheme will focus on reducing the horizontal orbit distortion. Scaling this measurement to the lowest energy operation of the storage ring (240 MeV), to achieve the tight tolerance set for the gamma-ray beam collimation established previously, our goal is to reduce the electron beam orbit displacement and angle at the collision point by a factor of about 2.5.

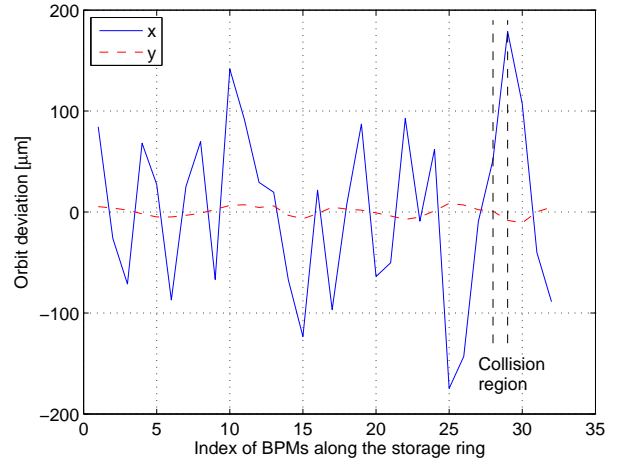


Fig. 3. (color online) Perturbed electron beam orbit along the storage ring. Measured with the storage ring energy $E_{SR} = 426$ MeV and the booster energy $E_{BST} = 1.2$ GeV.

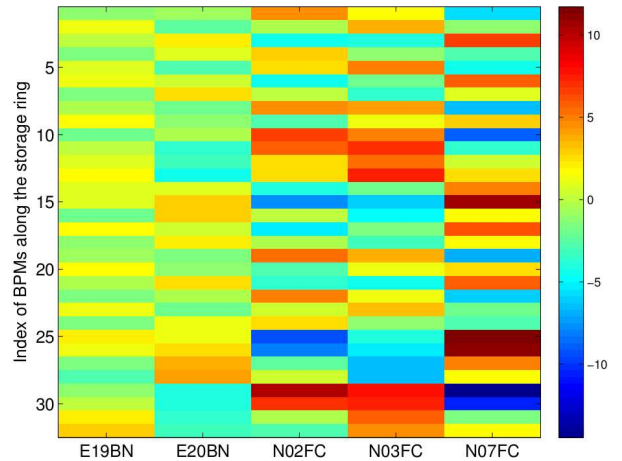


Fig. 4. (color online) Response matrix of a few selected correctors in the northeast section, measured with $E_{SR} = 426$ MeV, $E_{BST} = 500$ MeV.

With the booster ramped to the maximum energy of 1.2 GeV (Fig. 3), the effective kicking angle, assuming the orbit disturbance is localized, can be estimated to be about $\theta_0 \approx 20 \mu\text{rad}$ ($E_{SR} = 426 \text{ MeV}$), or an integrated field about $2.9 \times 10^{-5} \text{ T}\cdot\text{m}$ [13]. This correction is small, comparable to the strength of a typical corrector in the orbit feedback system. It is also noticed that the horizontal phase advance in the northeast area of the storage ring is $\Delta\mu_x \approx 0.6\pi$, therefore only a few correctors in this area are needed to minimize the orbit perturbation both inside and outside the area of the booster leakage field.

Five correctors in the northeast area of the storage ring are chosen as the candidates to compensate the localized booster leakage field. A beam based technique is used to determine the most effective combination of correctors. The response matrix for these correctors as shown in Fig. 4. Using the singular value decomposition (SVD) algorithm, the most effective eigenmode is found to be dominated by the N07FC and N02FC correctors. It is also known that these two correctors are separated by a betatron phase difference of 1.1π , which means they are almost equivalent but with opposite kicking angles. As the N07FC corrector is located further from the error source area, the N02FC corrector is clearly the better local corrector. In addition, a second corrector N03FC which has a 0.45π phase difference from N02FC is selected as the secondary corrector to reduce the residual orbit errors that N02FC is not capable of correcting.

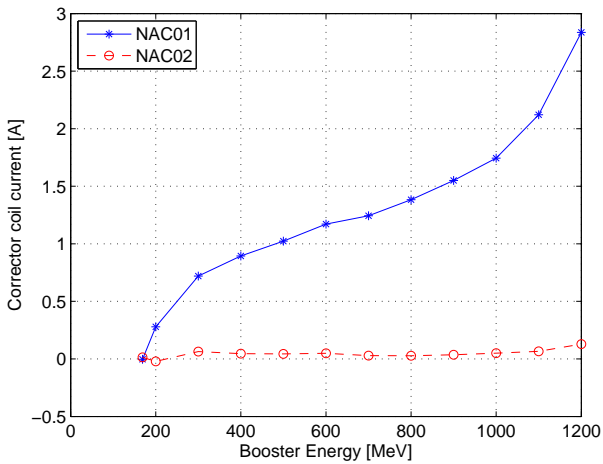


Fig. 5. (color online) Strengths of NAC01 and NAC02 measured with the booster injector parked at a set of energies between 169 and 1200 MeV. $E_{SR} = 426 \text{ MeV}$.

Since a typical booster energy ramping takes only 1.2 s, fast power supplies for the correctors are needed. A couple of ramping power supplies which are properly synchronized with the booster energy ramping are used to drive the N02FC and N03FC correctors. In the measurement it was found that the magnetic field produced

by these correctors has a time delay due to the induced eddy current in the soft-iron yoke. To overcome this problem, two dedicated air coil correctors NAC01 and NAC02 were developed and installed next to the N02FC and N03FC correctors, respectively, as shown in Fig. 1.

The strengths of the new correctors are determined with the booster injector parked at different energies (static mode), as shown in Fig. 5. It is clear that the strength of NAC01 is much larger than that of NAC02, which indicates that the booster leakage field is mostly local, therefore its main effect can be corrected using one local corrector NAC01. The maximum integrated field produced by NAC01 is estimated to be about $2.4 \times 10^{-5} \text{ T}\cdot\text{m}$, which is close to previously estimated value. It is observed that the strength of NAC01 is almost linear in the booster energy range from 300 MeV to 900 MeV, but in the low and high energy regions a nonlinear dependency on the booster energy shows up, which is likely resulted from the changed distribution of the leakage field. The compensation scheme is implemented in the EPICS based control system as a feedforward control, where the corrector strengths track the booster energy ramping.

3 Compensation results

To demonstrate the effectiveness of the compensation scheme, the uncompensated and compensated electron beam orbits in the storage ring are measured by the BPMs with the booster operated in both static and dynamic modes. Its usefulness is further confirmed using the direct measurements of the aiming stability of the undulator radiation.

Static mode

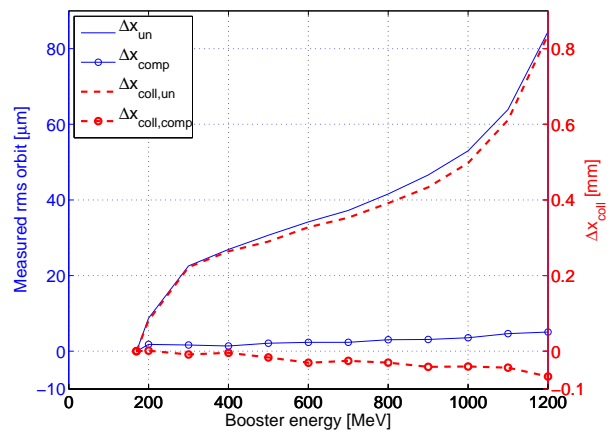


Fig. 6. (color online) The rms beam orbit change in the storage ring and the estimated gamma-ray center shift at the collimator as a function of the booster energy with the booster being operated in the static mode. Δx_{un} is the rms beam orbit measured without compensation and Δx_{comp} is the value with compensation. $\Delta x_{coll,un}$ is the

change of the gamma-ray beam center at the collimator without compensation, $\Delta x_{coll,comp}$ is the value with compensation. $E_{SR} = 426$ MeV.

As shown in Fig. 6, the beam orbit in the storage ring is measured using all BPMs around the storage ring with the booster operated in the static modes. The beam orbit offset Δx_c and angle $\Delta \theta_c$ at the collision point can be calculated using the two BPMs located at the either end of OK5-B and OK5-C undulator, respectively. Then the variations of the gamma-ray beam center at the collimator can be obtained using Eq. 1. It is observed that the trend of the storage ring rms orbit variation with the booster energy is very similar to the variation of the gamma-ray beam center at the collimator, which indicates a strong correlation between them. The measurement results show that in the static mode the compensation scheme reduces the maximum rms orbit variation by a factor of about 15, the same goes to the gamma-ray beam center variation, which is reduced from $840 \mu\text{m}$ to about $-67 \mu\text{m}$, well below the stability requirement for the HIGS operation (see in Section 2).

Dynamic mode

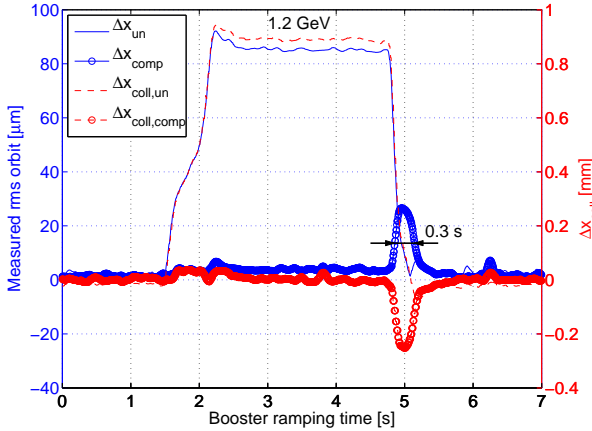


Fig. 7. (color online) The measured rms orbit distortions and estimated gamma-ray center variations at the collimator during a full booster ramp cycle. During the cycle, the booster is parked at 1.2 GeV for about 2.5 s (from $t = 2.2$ s to 4.7 s). $E_{SR} = 426$ MeV.

At the Duke storage ring, while the slow orbit feedback system uses the highly filtered low noise orbit data at a few Hz, the BPM acquisition system is capable of providing data at a higher rate of 30 Hz. The 30 Hz orbit data are fast enough to visualize the storage ring orbit changes during the 1.2 s booster energy ramp. As shown in Fig. 7, the beam orbit in the storage ring is measured for a complete booster ramping cycle. In this measurement, the booster starts its ramp from 169 MeV

at about $t = 1.4$ s and reaches the highest energy of 1.2 GeV at $t = 2.2$ s. After parking at 1.2 GeV for 2.5 s, it ramps down to 169 MeV in about 0.4 s. It is clear that the storage ring orbit stability is significantly improved along the booster ramp-up curve. The same is seen in the corresponding shift of the gamma-ray beam center. In the booster ramp-down process, a bump, with its peak about 30% of the uncompensated value, shows up in both curves. Even with this residual orbit bump during the booster energy ramp down, its amplitude is already small enough to satisfy the established goal for the compensation scheme (see Section 2). The duration of the residual bump is also much shorter than the time for the booster extraction (1 s to 2.5 s). The overall time-integrated orbit bump at the collision point is reduced by a factor of about 10 to 16 using this realtime feedforward field compensation, and the time-integrated gamma-ray perturbation on the collimator is reduced by a factor of about 14 to 25.

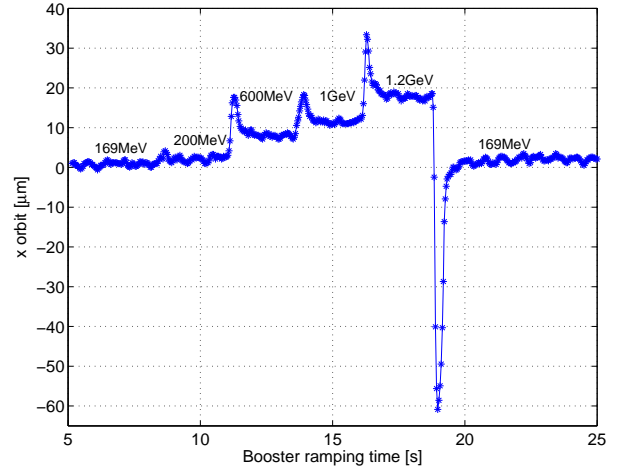


Fig. 8. (color online) Electron beam positions measured using the BPM at S07 sector with booster ramping. The beam orbit is measured with the booster ramped up in four discrete energy steps and parked at each energy for 2.5 s, and then ramped down to complete a cycle. As a reference, the uncompensated orbit at this location was about $+179 \mu\text{m}$ with the booster energy parked at 1.2 GeV. $E_{SR} = 426$ MeV.

The storage ring beam orbits were also measured with the booster energy ramped up from 169 MeV to 1.2 GeV in four discrete steps while parking at intermediate energies of 200 MeV, 600 MeV, 1 GeV, 1.2 GeV for 2.5 second each, and then ramped down to finish one cycle. The beam positions measured using the BPM at S07 sector (S07BPM) are shown in Fig. 8. It is observed that there is a small orbit peak during energy ramp-up and a small orbit shift after each ramp, both are the results of small under-correction. It is also observed that the beam orbit bump is reversed along the ramp-down process,

indicating orbit over-correction. These orbit peaks, either as under-correction during energy ramp-up, or over-correction during energy ramp-down, are the results of the delay in the field compensation system. While many factors can contribute to such delay, including the finite time response of the control system and corrector power supplies, the most likely factor is the eddy current effect in the thick storage ring vacuum chamber (3 mm, stainless steel).

Direct measurement of undulator radiation aiming

Beam orbit stability in the south straight section is further verified by directly measuring the stability of the FEL undulator radiation aiming. The OK5-B and OK5-C undulators located adjacent to the Compton collision point are turned on and set to a fixed current to produce synchrotron radiation. The undulator photon beam (center wavelength $\lambda_{cen} = 550$ nm, $E_{SR} = 426$ MeV) is measured using a beam profile monitor located about 30 m downstream from the Compton collision point. The CCD camera in the monitor is capable of taking about 14 frames per second in the burst mode. Due to the long distance between the radiation source and the camera, the variation of the undulator beam image center at the camera is mainly caused by the change of the electron beam angle in the undulators. In this measurement, a bandpass optical filter is used to reduce the background radiation.

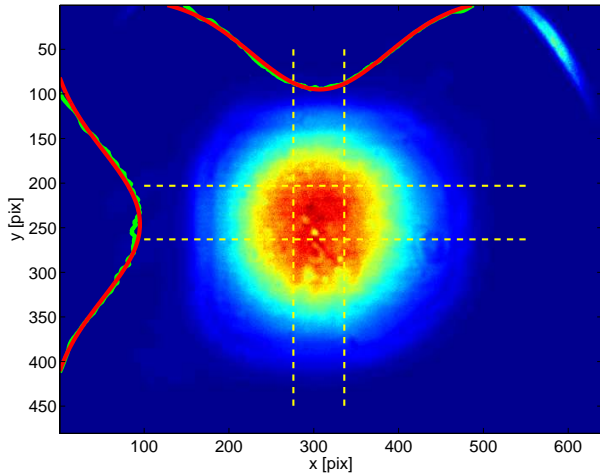


Fig. 9. (color online) Measured FEL undulator radiation beam image with center wavelength $\lambda_{cen} = 550$ nm. The beam image centers are fitted with Gaussian functions using the intensity distribution within the selected areas. The yellow dash-lines: the boundaries of the selected areas; green dot-lines: the intensity distribution of the data in the selected areas; red lines: the fitted curve of the intensity distribution. $E_{SR} = 426$ MeV.

The image data are processed first by subtracting the background noise, and the image center is found by fit-

ting the intensity distribution of a selected area in the horizontal or vertical direction using a Gaussian function, as shown in Fig. 9. Hence, the beam images can be recorded with the booster operated in the dynamic mode. The measurement results with booster ramping in a full cycle, before and after compensation, are shown in Fig. 10. Without compensation, the average perturbation of the image center is about $770 \mu\text{m}$ (average over measurements between $t = 4.1$ s and $t = 6.6$ s) when the booster is parked at 1.2 GeV. This value is significantly reduced to about $-3 \mu\text{m}$ (average) with the compensation, which is within the level of the rms noise ($58 \mu\text{m}$, from data between $t = 0$ to 2 s and $t = 8$ to 10 s when the booster is operated at the lowest energy of 169 MeV). Along the booster ramp-down process, a small but visible bump shows up in the negative direction. The height of this peak is about 1/4 of the uncompensated value with the booster operated at 1.2 GeV, which is consistent with the previous BPM measurement result.

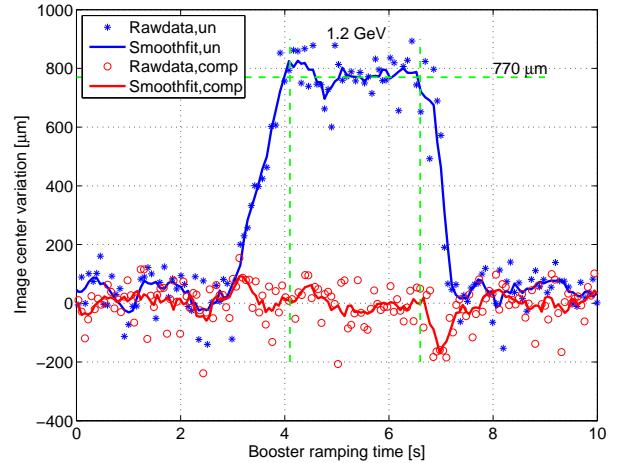


Fig. 10. (color online) Variations of undulator radiation image center measured using a beam profile monitor during a full booster ramp cycle, the booster is parked at 1.2 GeV for about 2.5 s as in Fig. 7. Blue stars are the measured beam centers without compensation; red-circles are those measured with compensation; blue-line and red-line are the smoothed curves using a 5-point moving average. $E_{SR} = 426$ MeV.

4 Summary and discussion

The stability of the electron beam orbit is a critical requirement for the HIGS operation at the Duke storage ring. To keep the aiming of the gamma-ray beam stable, therefore to maintain the energy resolution of the highly collimated gamma-ray beam, the e-beam orbit distortion in the storage ring, especially at the Compton collision point, needs to be minimized. In the development of the compensation scheme for the booster leakage field, two

effective correctors are chosen using the beam based technique. Faster air coil correctors without steel yokes are developed and installed, and their strengths for orbit correction are determined by stepping the booster through a set of energies between 169 MeV and 1.2 GeV. The field compensation is implemented as a feedforward in the realtime booster control system.

With this compensation scheme, the maximum perturbation of the horizontal beam orbit and gamma-ray beam aiming is significantly decreased by a factor of 3 with the booster operated in the ramping mode. In the routine operation, the overall time-integrated distortion in the gamma-ray beam aiming is expected to be decreased by a factor of 14 to 25. The projected maximum horizontal gamma-ray beam center shift at the collimator is reduced from 1677 μm to 447 μm (about 340 μm in the vertical without the need for compensation) with booster ramping and for the lowest energy operation of

the storage ring (240 MeV). This value is about 7% of the smallest collimator diameter ($D = 6$ mm), well below our preliminary goal of 10%. We plan to improve the orbit compensation during the booster ramp-down process. Instead of using energy-indexed corrector settings measured by stepping up the booster, a new set of settings will be determined by stepping down the booster energy.

We would like to thank the engineering and technical staff at DFELL/TUNL for their support of this research work. This work was supported by National Natural Science Foundation of China (No. 11175180, 11475167) and DOE Grant (No. DE-FG02-97ER41033). One of the authors (Wei Li) also would like to thank the China Scholarship Council (CSC) for supporting his research visit at Duke University.

References

- 1 S.F. Mikhailov, et al, Commissioning of the booster injector synchrotron for the HIGS facility at Duke university, Proceedings of the PAC07 (2007).
- 2 S.F. Mikhailov, et al, Multi-bunch injection scheme for the duke booster synchrotron for top-off injection, Proceedings of the PAC09 (2009).
- 3 Y.K. Wu, et al, Phys. Rev. Lett., **96**: 224801 (2006).
- 4 V.N. Litvinenko, J.M.J. Madey, Nucl.Instr.Meth. in Phys. Res. Sect. A, **375**: 580-583 (1996).
- 5 V.N. Litvinenko, et al, Phys.Rev.Lett, **78**: 4569 (1997).
- 6 W. Joho et al, Nucl. Instrum. Methods A, **562**(1): 1-11 (2006).
- 7 H.J Tsai et al, Hardware Improvements and Beam Commissioning of the Booster Ring in Taiwan Photon Source, Proceeding of IPAC2015, Richmond, USA (2015).
- 8 R. Keller et al, Orbit stability of the ALS storage ring, Proceeding of PAC1997, **1**:784-786 (1997).
- 9 M. Eriksson et al, J. Synchrotron Radiat., **21**(5): 837-842 (2014).
- 10 Y.K. Wu, et al, Performance and Capabilities of Upgraded High Intensity Gamma-ray Source at Duke University, Proceedings of the PAC09 (2009).
- 11 Y.K. Wu, et al, BPM and orbit correction systems at the Duke storage ring, Proceedings of the PAC03, **4**: 2479-2481 (2003).
- 12 M. Böge, et al, Fast Closed Orbit Control in the SLS Storage Ring, Proceedings of the PAC1999, **2**: 1129-1131 (1999).
- 13 S.Y Lee, Accelerator physics (World Scientific, 2004).